

# The Visual Orbit of $\theta^2$ Tauri and the Distance to the Hyades

Xiaopei Pan<sup>1</sup>, Michael Shao<sup>2</sup>, Shri Kulkarni<sup>3</sup>

Received \_\_\_\_\_; accepted \_\_\_\_\_

---

<sup>1</sup>UTA, Inc., 283 S. Lake Ave., Pasadena, CA 91101

<sup>2</sup>Jet Propulsion Laboratory, California Institute of Technology, 4800 Oak Grove,  
Pasadena, CA 91109

<sup>3</sup>California Institute of Technology, 1201 California Blvd., Pasadena, CA 91125

## ABSTRACT

We report on ten years' interferometric observations at multiple wavelengths of  $\theta^2$  Tauri, the brightest star of the Hyades cluster. The visual orbit of this high-eccentricity spectroscopic binary system has been determined independently from the interferometric observations. The inclination is determined as  $47^\circ.3 \pm 0^\circ.9$  with a semi-major axis of  $19.15 \pm 0.25$  mas, and maximum and minimum separations of 27 mas and 3.7 mas, respectively. The longitude of the periastron,  $\omega$ , is determined as  $56^\circ.0 \pm 1^\circ.2$ . The luminosities of the two components are determined as  $3.73 \pm 0.04$  mag and  $4.83 \pm 0.08$  mag at V band, respectively. These results are consistent with the projected minimum separations determined from lunar occultation measurements.

Combining interferometric measurements with the latest spectroscopic observations yields masses of the two components of  $2.30 \pm 0.29 M_\odot$  and  $2.01 \pm 0.16 M_\odot$ , respectively. The orbital distance of  $\theta^2$  Tauri is determined as  $45.0 \pm 1.6$  pc, consistent with the corresponding distance from Hipparcos of  $45.68 \pm 1.73$  pc. Since  $\theta^2$  Tauri is only 0.6 pc in front of the center of the Hyades cluster, the distance modulus of the Hyades is obtained as  $3.30 \pm 0.08$  mag. Comparisons of measurements from interferometry, spectroscopy, precision photometry, lunar occultation, and Hipparcos not only checks the accuracy of the distance to the Hyades, but also provides an accurate empirical mass-luminosity relation, and a good estimate of the age of the Hyades.

*Subject headings:* binaries: visual - instrumentation: interferometers  
- stars: individual ( $\theta^2$  Tauri)

## 1. Introduction

The brightest and the most massive main-sequence star in the Hyades cluster,  $\theta^2$  Tauri, has attracted repeated observations by many different techniques including spectroscopy, lunar occultation, Hipparcos, and visual and infrared interferometry, not only because the object is of significant importance in astrophysics, but also because it is a challenging task to measure it. Almost one hundred years of hard work on  $\theta^2$  Tauri has been done by several generations of astronomers, and it is now time to gather all of measurements to draw the best physical picture of the system.

Early spectroscopic observations (Moore 1908; Frost 1909) revealed the binary nature of this system. Further investigation (Plaskett 1915; Petie 1940; Ebbighausen 1959) obtained three sets of orbital parameters of gradually improving accuracy. In the Eighth Catalogue of the Orbital Elements of Spectroscopic Binary Systems (Batten et al. 1989) the orbit of  $\theta^2$  Tauri is classified as type “b”, which is better than average, but not definitive. Because both components of this system are fast rotators with velocity of more than 100 km/s, none of these three investigations had been able to detect the secondary spectrum. In addition, the differences among their values of space velocity ( $\nu_0$ ) led to suspicions of the existence of a third body (Plaskett 1915).

Only in the 1990’s was extensive effort made on this important system. Three key aspects have been improved in recent spectroscopy.

First, the companion’s spectra were detected twice, and only twice (Peterson et al. 1993; Tomken et al. 1995). It is extremely difficult to extract reliable velocities of the companion because of line broadening. Only near periastron passage, which has the maximum velocity differences between the two components, can the spectra of the companion be clearly identified.

Second, the semi-amplitude of the radial velocity of the primary ( $K_1$ ) is improved significantly. Although the companion's spectra were masked by the primary for more than 80 years, the primary's spectra are distorted by the companion via the "pulling effect" (Torres et al. 1997). The estimated value and accuracy of  $K_1$  has steadily increased with later observations.  $K_1$  was estimated as about  $27 \pm 1.4$  km/s from 1915 to 1940, about  $30 \pm 0.6$  km/s during 1959 - 1995, and is currently estimated as  $33 \pm 0.4$  km/s. New observing techniques and better algorithms made the improvement possible.

Third, the estimated value of  $\nu_0$  is stabilized at about 39 km/s. It is now clear that there is no third body in this system.

In astrometry, the minimum separation and magnitude difference of this spectroscopic binary were determined by lunar occultation (Evans and Edwards 1980; Peterson et al. 1981). The true separations of this system were determined by the Mark III Optical Interferometer (Shao et al. 1988) on Mt. Wilson and preliminary visual orbits were published (Pan et al. 1992b; Hummel and Armstrong 1992). Because of limited time coverage of the observations, these interferometric solutions of the orbit depended on three parameters (P, T, e) from spectroscopy, whose values have been significantly improved recently. On the other hand, spectroscopic studies of that system (Torres et al. 1997) used these preliminary results from interferometers in their data analysis. Thus two types of data analysis affected each other, and could not incorporate the best parameters from each other. A series of new observation of  $\theta^2$  Tauri was made with the Palomar Testbed Interferometer (Colavita et al. 1999b) in 1998, so that a total of ten years' interferometric results at different wavelengths are available now.

The purpose of this paper is to present observational results from both the Mark III and the PTI interferometers in detail. The visual orbit and photometry of  $\theta^2$  Tauri are determined accurately and independently using the interferometric data. Comparisons

among different methods, including spectroscopy, interferometry, lunar occultation, precision photometry, and Hipparcos, are conducted. Combining results from all techniques, the distance to the Hyades and precise mass-luminosity relations are provided.

## 2. Observations and data analysis

The star  $\theta^2$  Tauri (HR 1412, HD 28319,  $R.A. = 4^h28^m$ ,  $Decl. = 15^\circ52'$  for equinox J2000.0) is a double-line spectroscopic binary of 3.40 mag at V band. The listed wider companion,  $\theta^1$  Tauri, is  $340''$  away in the sky. The primary (A7III) is the most massive main-sequence star in the Hyades, and is located at the critical turnoff region on the evolution tracks. Extensive photometric studies reveal that the primary is a  $\delta$  Scuti type of variable star, which has a pulsation amplitude of 0.013 mag (peak-to-peak) and frequencies of 13–15 cycles per day (Breger et al. 1980). The primary has a fast rotation velocity of 100 km/s (Tomken et al. 1995), while the companion rotates more rapidly with velocity of approximately 150 km/s (Torres et al. 1997)

Observations of  $\theta^2$  Tauri with the Mark III Optical Interferometer were made during 1989–1990 using variable baselines oriented in the direction of North-South. The resolution of the instrument depends on the length of the projected baseline, which varied from 3.0 to 31.5 m. One white-light channel was used for fringe tracking, and three narrow-band channels were used for visibility measurements at 800, 550 and 450(500 in 1990) nm with bandwidths of 25 nm. The aperture for the narrow-band channels was 2.5 cm. During observation of a star, each scan included 75 s of fringe tracking and a 5 s measurement of dark count and sky background. Further details on data analysis with the Mark III Optical Interferometer can be found elsewhere (Pan et al. 1992a).

The Palomar Testbed Interferometer has a fixed baseline of 110 m and effective

aperture of 40 cm. The observations reported here were at wavelength of 2.2  $\mu\text{m}$ . The instrument uses path-length modulation and synchronous demodulation for the fringe detection, which is similar to the Mark III Optical Interferometer. A NICMOS-3 infrared array is used for detection of fringes in a white-light channel and 5 spectral channels with bandwidths of  $\approx 65$  nm. Incoherent visibility estimators with bias corrections are averaged over typically 130 s of fringe tracking (Colavita 1999a). Fully automated observations take about 6 minutes for each scan.

In order to calibrate the systematic visibility biases, reference stars with diameters of 1 mas or less are used. For a baseline of 110 m on PTI the squared visibility of stars with diameters of 0.5, 0.75 and 1 mas are 0.96, 0.92, and 0.86, respectively. During the course of the observation several calibration stars are observed periodically. The system visibility  $V_s^2$  is computed as:

$$V_s^2 = V_m^2/V^2(\theta, \lambda, B_p), \quad (1)$$

where  $V_m^2$  is the average value of visibility squared, and the theoretical  $V^2$  is estimated from the angular diameter of the calibrator, wavelength, and the length of the projected baseline. The calibrated visibility squared of the target star is calculated as:

$$V_t^2 = V_m^2/V_s^2. \quad (2)$$

The fringe visibility squared of a binary star can be described (Pan et al. 1992a) as

$$V^2 = F(\mathbf{d}, \lambda, r, S_r, S_d, \theta_1, \theta_2), \quad (3)$$

where  $\mathbf{d}$  is the projected baseline vector,  $\lambda$  is the observing wavelength,  $r$  is the intensity ratio between two components,  $S_r$  and  $S_d$  are the separations between the two components in the direction of R.A. and Decl., and  $\theta_1$  and  $\theta_2$  are the angular diameters of the components. A nonlinear model fitting algorithm is applied to the calibrated squared fringe visibilities for each night.

We have nine nights of observations on the Mark III interferometer during 1989–1990 with baseline lengths of 15.13 to 31.5m for observation of  $\theta^2$  Tauri. This is a highly eccentric system, and the companion stays in the south-west quadrant for most of time—almost 75% of the duration of its period—while in 35 days the position angle of the companion changes by  $270^\circ$ . In order to well constrain the orbit determination, we made special effort to obtain well-spaced observations on PTI, and achieved good observations near periastron. In 1998, six nights of observation on PTI covered a range of  $280^\circ$  in position angles, including one night very close to the minimum separation of 4 mas.

The observation journal is listed in Table 1. Typical plots of fringe visibilities vs. model fitting are presented in Figs. 1–3 for the Mark III Interferometer. A typical plot at K band for PTI is shown in Fig. 4. Because of the small magnitude differences (about 1.1 mag), and large separations (most about 20 mas), it is not difficult to obtain accurate separations and intensity ratios from interferometry. Since both components have similar colors, the measurement precisions at different wavelengths are similar. While the fast rotation of both components has made spectroscopic measurements difficult, this is not an issue for the interferometric observations.

### 3. Visual Orbit and Precision Photometry

The visual orbit of  $\theta^2$  Tauri (Fig. 5) is determined by a least squares method (Pan et al. 1992a). The residuals between measured and calculated separations (M-C) in Table 2 are approximately 0.2 mas, which reflects the external precision of the visibility measurements. All seven orbital parameters can be obtained just from interferometric measurements, and are listed in the last column in Table 3. This allows direct comparisons between interferometric and spectroscopic observations. Although the values of period from different radial velocity measurements and interferometric measurement agree with each

other to their claimed accuracy, the values of eccentricity and the longitude of periastron determined from different spectroscopic observations are quite different. In particular, the widely used eccentricity of  $0.750 \pm 0.006$  from (Ebbighausen 1959) has a  $4\sigma$  offset, and  $\omega$  has almost a  $6\sigma$  difference, when compared with the most recent spectroscopic results (Torres et al. 1997). The differences among different spectroscopic measurements has an important impact for determination of the physical parameters of the system. Compared with the most recent spectroscopic results, use of the old value for the eccentricity causes a 4% systematic bias in the distance to the star, and causes an 8% change in the estimate of mass. Unfortunately, we used that old value ( $e = 0.750$ ) to obtain  $a''$ ,  $i$ ,  $\omega$ , and  $\Omega$  in our preliminary orbit (Pan et al. 1992a). Those inaccurate  $a''$  and  $i$  then were used by later spectroscopic data analyses (Peterson et al. 1993; Tomken et al. 1995; Torres et al. 1997). Now we have two sets of orbital parameters from spectroscopy and interferometry separately and independently. The latest set of orbital parameters from spectroscopy (Torres et al. 1997) agree with those from interferometry to  $2\sigma$ . The significant improvement in the spectroscopic results came from the consideration of the companion's "pulling effect", which introduced distortion in the primary's radial velocities as high as 4 km/s. The results from interferometry confirm the effectiveness of the two-dimensional cross-correlation technique in spectroscopy. It can now be concluded that for the two common parameters between spectroscopy and interferometry, the eccentricity must be 0.73, not 0.75; and  $\omega$  must be  $56^\circ$ , not  $49^\circ$ . We combined two data sets from spectroscopy (Tomken et al. 1995; Torres et al. 1997) and interferometry (this work), and used the best estimates of orbital parameters for calculation of physical parameters.

The Hyades main-sequence stars play a fundamental role in astronomy to determine the cosmological distance scale. The main-sequence fitting method depends on the locations of the Hyades stars on the H-R diagram. Thus precise photometric parameters of stars are critical, particularly for binary stars. At present long baseline interferometry is the only



technique which can provide accurate magnitude differences for close pairs at separations of milli-arcseconds. For the case of  $\theta^2$  Tauri, intensity ratios at four bandwidths from blue to near-infrared are obtained as shown in Table 4. The magnitude differences for different bands are the weighted average values from multiple nights of observations. From the luminosity and color index of the companion it is obvious that the companion is an A5 V type of main sequence star.

It is useful to compare interferometric results with the measurements from lunar occultation (Peterson et al. 1981; Evans and Edwards 1980). Despite its difficulty in making repeated measurements, lunar occultation provides high resolution angular measurements and high precision photometry for binaries with small separations. Although only projected separations in a direction perpendicular to limb motion can be measured from lunar occultation, those measurements can be compared with calculated values from the interferometric orbit, and serve as an external check of measurement accuracies for both techniques. A valuable fact is that angular measurements from lunar occultation do not have  $180^\circ$  ambiguities. For  $\theta^2$  Tauri the angular separations and magnitude differences from lunar occultation and interferometry are listed in Table 5. It can be seen that the best occultation measurements are consistent with interferometric results to a precision of 1 mas for separation and 1% for magnitude differences.

#### 4. Distance to the Hyades and Mass-Luminosity Relation

It is common practice to incorporate the angular size of the orbit from interferometry with linear size from spectroscopy to determine orbital parallax. The difficulty for  $\theta^2$  Tauri is that the companion's radial velocities can be obtained only near periastron, and have had large uncertainties. A value of  $38 \pm 2$  km/s (Tomken et al. 1995; Torres et al. 1997) is adopted here. Also, the latest value of the primary's radial velocity of  $33 \pm 0.39$  km/s

(Torres et al. 1997) , which is free of contaminations from the companion, is adopted. In this case the distance to the system is determined as  $45.0 \pm 1.6$  pc with a corresponding orbital parallax of  $22.21 \pm 0.79$  mas. This result is in excellent agreement with the Hipparcos parallax of  $21.89 \pm 0.83$  mas, or  $45.68 \pm 1.73$  pc.

In the central 2 pc region of the Hyades cluster, only stars more massive than about  $1M_{\odot}$  are found (Brown et al. 1997), and most of them are binaries. In fact,  $\theta^2$  Tauri is the most massive main-sequence star, and is located very near the center. By using proper motions, the relative distance of  $\theta^2$  Tauri to the center of the Hyades is determined as  $0.6 \pm 0.1$  pc by both the Hiparcos catalogue (Brown et al. 1997), and the FK5 and PPM catalogues (Schwan 1991). The distance to the Hyades based on  $\theta^2$  Tauri is obtained as  $45.6 \pm 1.6$  pc, corresponding to a distance modulus (m-M) of  $3.30 \pm 0.08$  mag. The Hipparcos distance to the Hyades is  $46.34 \pm 0.27$  pc, or a distance modulus of  $3.33 \pm 0.01$  mag (Brown et al. 1997).

Combination of both interferometric and spectroscopic measurements also lead to determination of the masses as  $M_1 = 2.30 \pm 0.29M_{\odot}$  and  $M_2 = 2.01 \pm 0.16M_{\odot}$ , respectively.

By applying bolometric corrections for both components,  $-0.01 \pm 0.01$  mag for the A3 III primary, and  $-0.02 \pm 0.01$  mag for the A5 V companion, the absolute bolometric magnitudes for components are determined as  $0.46 \pm 0.04$  mag and  $1.56 \pm 0.05$  mag, respectively. The color index for the primary is  $0.18 \pm 0.02$  mag for (B-V) and  $0.48 \pm 0.02$  mag for (V-K). The color index for the companion is  $0.15 \pm 0.02$  mag for (B-V) and  $0.46 \pm 0.02$  mag for (V-K). As expected, the companion, as a main sequence star, fits to the main-sequence isochrones exactly. However, the primary has evolved off the main-sequence, and is above the turnoff region. The primary's location on the M-L diagram and on the C-M diagram are consistently fit to the isochrones with a age of about 600 Myrs. The primary is at the end of the core hydrogen burning phase.

## 5. Summary

We have analyzed ten years' interferometric observations of  $\theta^2$  Tauri, and derived an independent visual orbit and precise photometric parameters. Our results are consistent with those from lunar occultation, spectroscopy and Hipparcos. These new determinations provide accurate distance and luminosity information for the critical star  $\theta^2$  Tauri, which can be used to help determine the age of the Hyades. It would be desirable to have better than 2% precisions for the distance to the Hyades and masses of both components. In fact orbital parameters from interferometry all have precisions of 1-2 %, the uncertainty of distance and masses would be improved if the precision of the spectroscopic measurements could reach 2%, which is common in spectroscopic measurements.

Thanks to Mark Colavita for many useful comments and a careful reading of the manuscript. This work was supported by NASA under its Origins Program. Interferometer data was obtained at the Palomar Observatory using the NASA Palomar Testbed Interferometer, which is supported by NASA contracts to the Jet Propulsion Laboratory. Science operations with PTI are conducted through the PTI collaboration (<http://huey.jpl.nasa.gov/palomar/ptimembers.html>). Other interferometer data was obtained with the Mark III Interferometer, which was operated by the Naval Research Laboratory with funding from the Office of Naval Research. Literature survey is based on the SIMBAD system.

## REFERENCES

- Batten, A. H., Fletcher, J. M. and MacCarthy, D. G. 1989, *Publ. Dom. Astrophys. Obs.*, 17, 10.
- Breger, M., Lin, Huang, Shi-yang, Jiang, Zi-he, Guo, Antonello, E. and Mantegazza, L. 1987, *A&A*, 175, 117
- Brown, A.G.A., Perryman, M.A.C., Kovalevsky, J., Robichon, N., Turon, C., Mermilliod, J.-C. 1997, *Proc. ESA SP-402*, 681
- Colavita, M. M. 1999, *PASP*, 30, 111
- Colavita, M. M., Wallace, J. K., Hines, B. E., Gursel, Y., Malbet, F., Pan, X. P., Shao, M., Yu, J. W., Boden, A. F., Dumont, P. J., Gubler, J., Koresko, C. D., Kulkarni, S. R., Lane, B. F., Mobley, D.W. and van Belle, G. T. 1999, *ApJ*, 510, 505
- Ebbighausen, E. G. 1959, *Publ. Dom. Astrophys. Obs.*, 11, No. 9, 235
- Evans, D. S. and Edwards, D. 1980, *Observatory*, 100, 206
- Frost, E. B. 1909, *ApJ*, 29, 237
- Johnson, H. L., Mitchell, R. I., Iriarte, B., and Wisniewski, W. Z. 1966, *Pub. Lunar and Planet. Lab., Univ. Ariz.*, 4, 99.
- Hummel, C. A. and Armstrong, J. T. 1992, *IAU Coll. 135*, 552
- Moore, J. H. 1908, *Lick. O.B.*, No. 146, 1
- Pan, X.P., Shao, M., Colavita, M. M., Armstrong, J. T., Mozurkewich, D., ViVekanand, M., Denison, C. S., Simon, R. S., and Johnston, K. J. 1992, *ApJ*, 384, No.2, 624.
- Pan, X.P., Shao, M and Colavita, M. M. 1992, *IAU Coll. 135*, 502

Plaskett, J. S. 1915, Publ. Dom. Obs., 2, 63

Peterson, D. M., Baron, R. L., Dunham, E. and Mink, D. 1981, AJ, 86, 1090

Peterson, D. M., Stefanik, R.P. and Latham, D. W. 1993, AJ, 105, 2260

Petrie, R. M. 1940, PASP, 52, 286

Shao, M., Colavita, M. M., Hines, B. E., Staelin, D. H., Hutter, D. J., Johnston, K. J.,  
Mozurkewich, D., Simon, R. S., Hershey, J. L., Hughes, J. A. and Kaplan, G. H.  
1988, A&A, 193, 357.

Schwan 1991, A&A, 243, 386

Tomkin, J., Pan, X. P. and McCarthy, J. K. 1995, AJ, 109, 780

Torres, G., Stefanik, R. P. and Latham, D. W. 1997, ApJ, 485, 167

Fig. 1.— Measured and best-fit visibilities For  $\theta^2$  Tauri at 800 nm from the Mark III interferometer, 1989 November 2. The errors of each scan ( $\pm 1\sigma$ ) are indicated by vertical lines around the measured data. The best fit curve corresponds to magnitude difference of 1.1 mag, and separations in R.A. and Decl. of -17.57 mas and -16.17 mas, respectively.

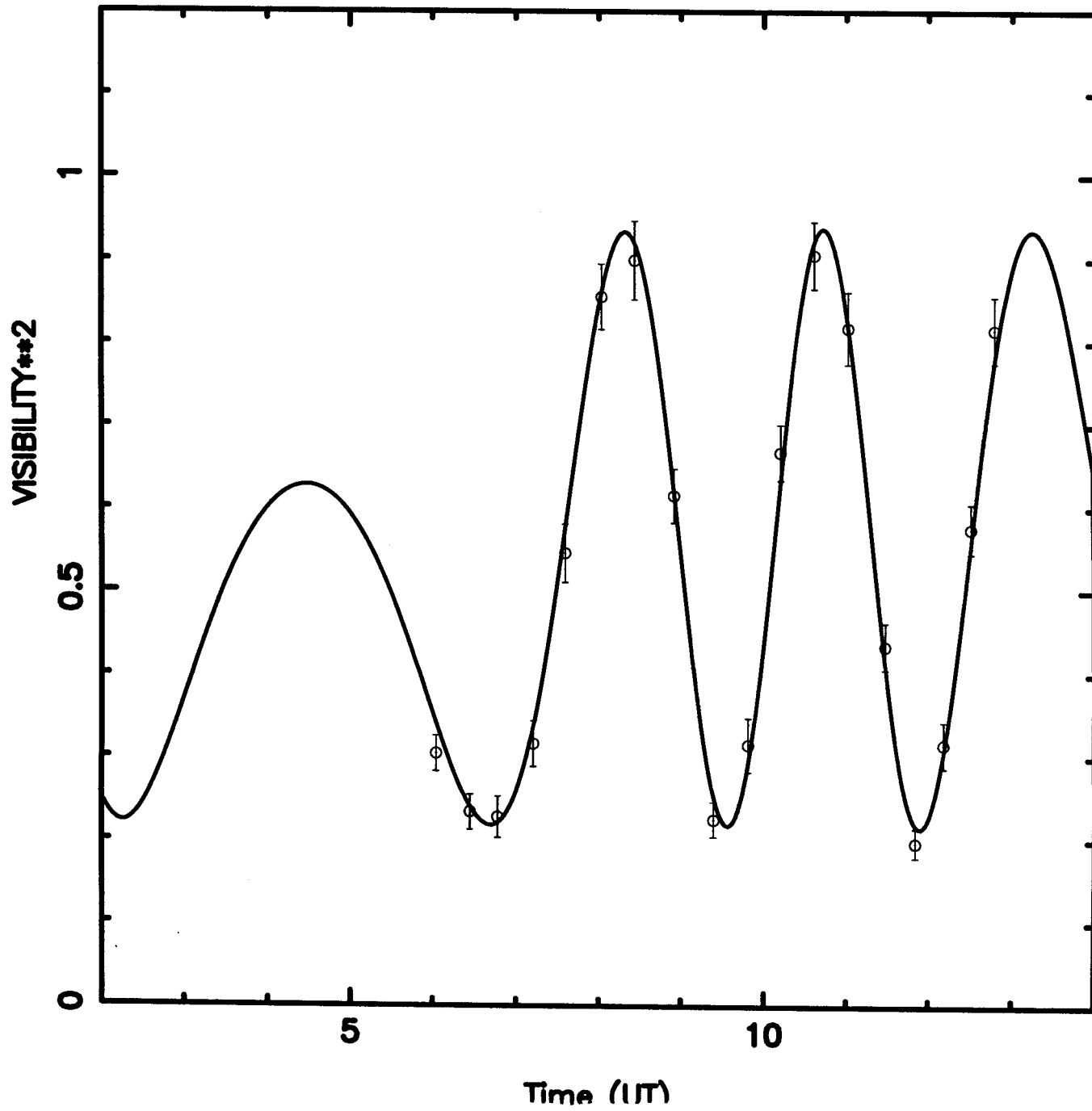
Fig. 2.— Measured and best-fit visibilities For  $\theta^2$  Tauri at 550 nm from the Mark III interferometer, 1989 November 2. The errors of each scan ( $\pm 1\sigma$ ) are indicated by vertical lines around the measured data. The best fit curve corresponds to magnitude difference of 1.0 mag, and separations in R.A. and Decl. of -17.81 mas and -16.24 mas, respectively.

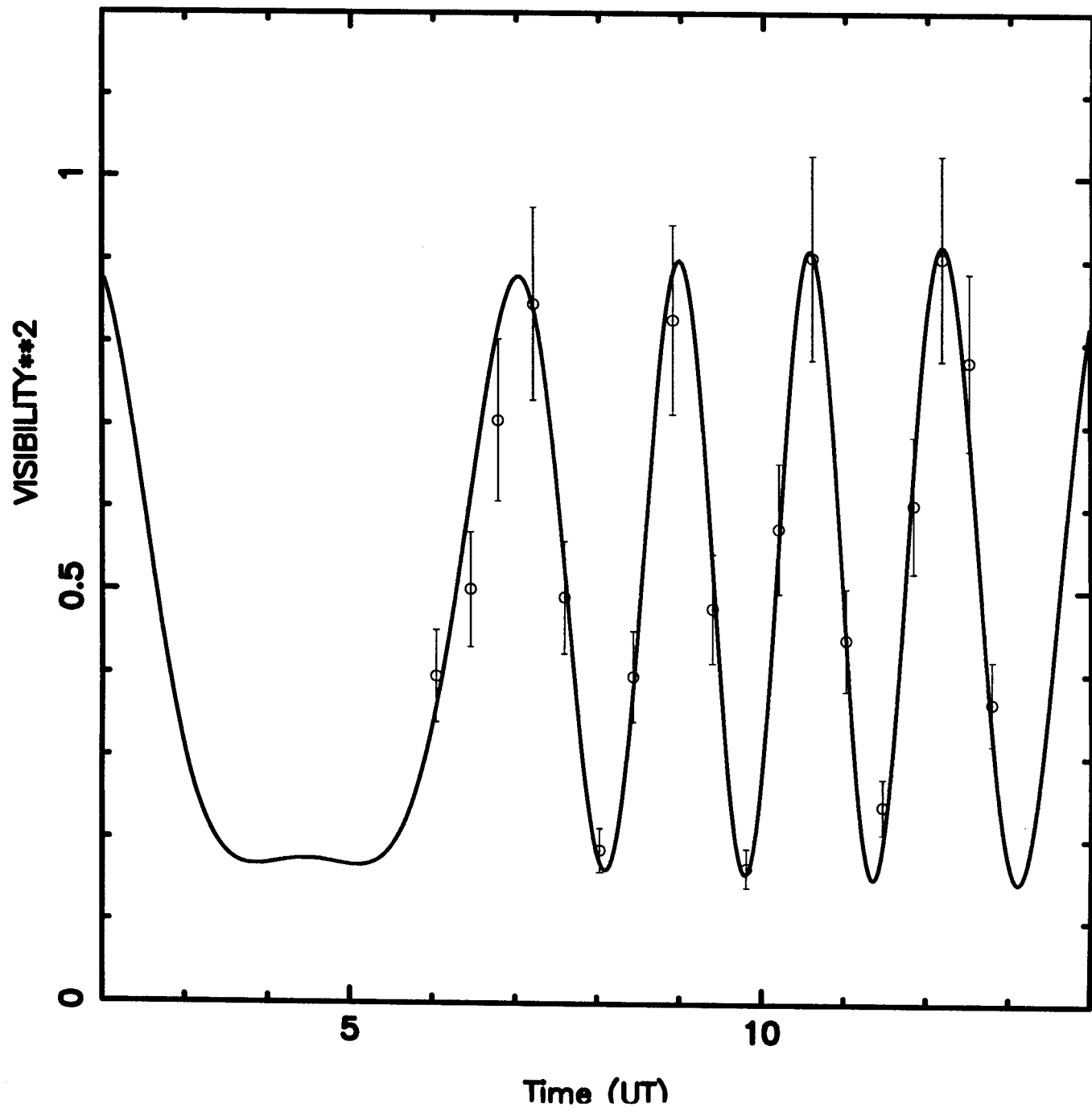
Fig. 3.— Measured and best-fit visibilities For  $\theta^2$  Tauri at 450 nm from the Mark III interferometer, 1989 November 2. The errors of each scan ( $\pm 1\sigma$ ) are indicated by vertical

lines around the measured data. The best fit curve corresponds to magnitude difference of 1.0 mag, and separations in R.A. and Decl. of -17.98 mas and -16.14 mas, respectively.

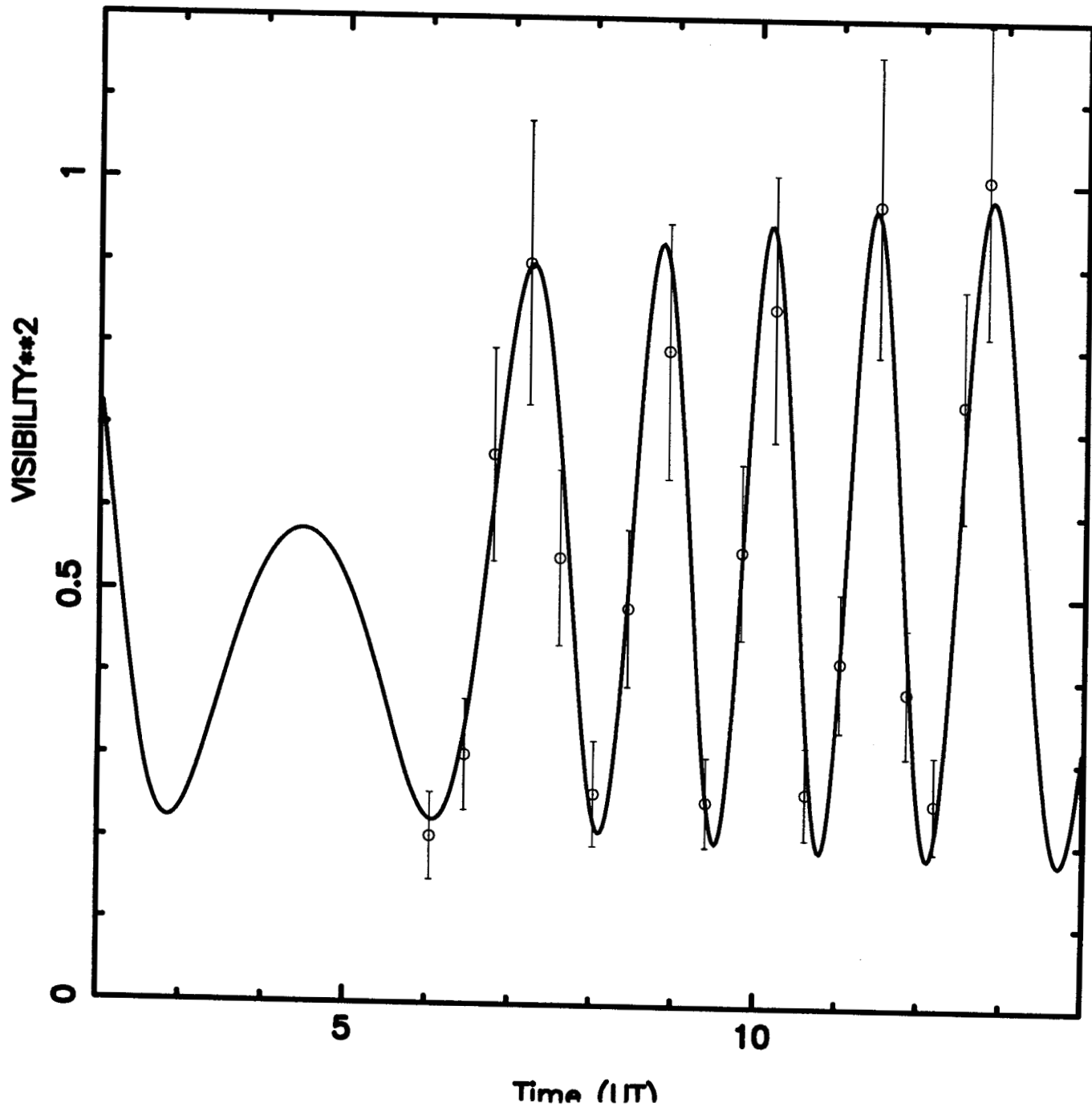
Fig. 4.— Measured and best-fit visibilities For  $\theta^2$  Tauri at  $2.2 \mu\text{m}$  on PTI, 1998, October 18. The errors of each scan ( $\pm 1\sigma$ ) are indicated by vertical lines around the measured data. The best fit curve corresponds to magnitude difference of 1.2 mag, and separations in R.A. and Decl. of -14.1 mas and 0.17 mas, respectively.

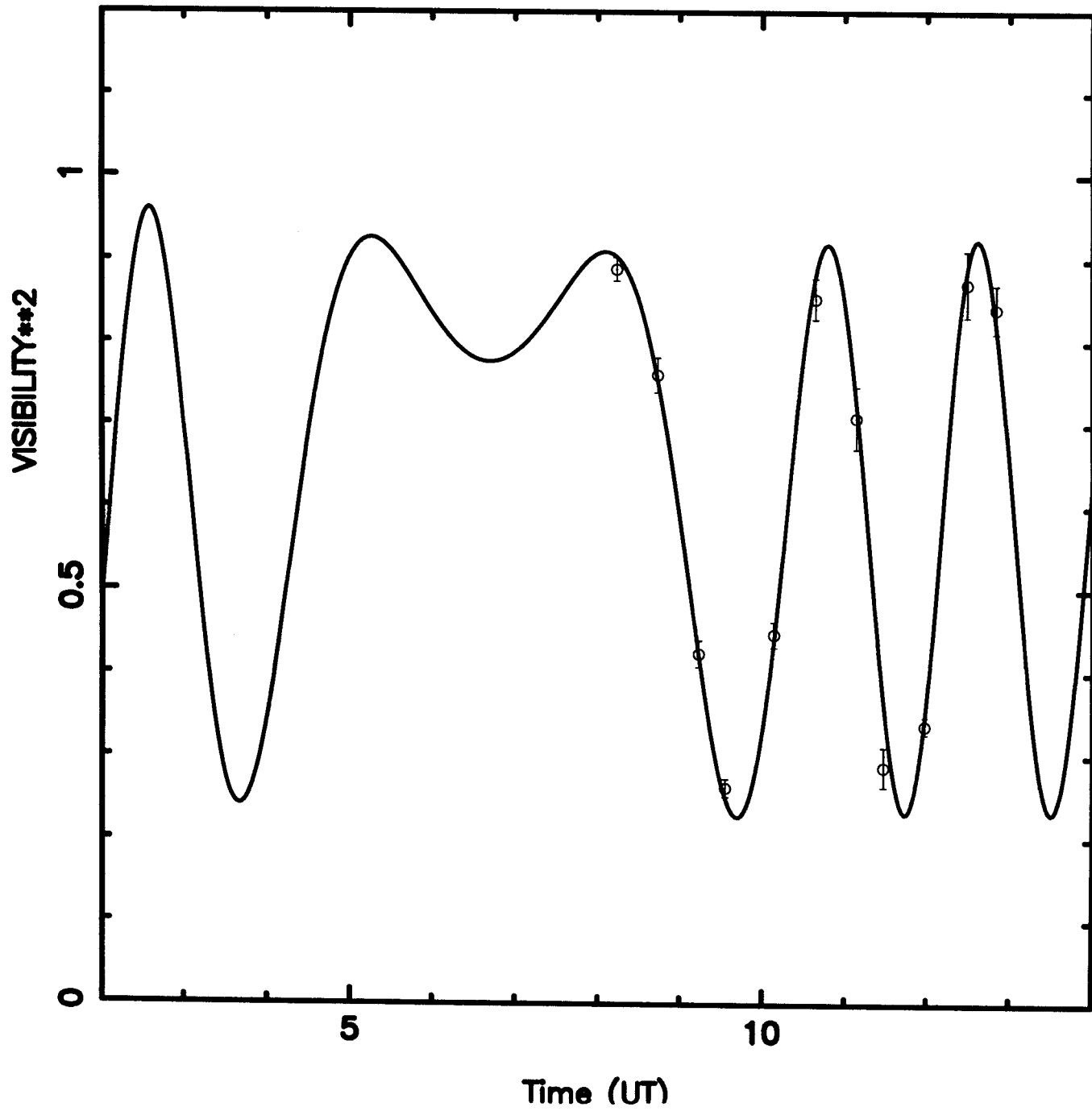
Fig. 5.— Measured data and visual orbit. The individual measurements, which are at the center of the open triangles, are connected to the calculated positions by a short line. The formal errors ( $\pm 1\sigma$ ) in R.A. and Decl. are indicated by the lengths of crosses centered on the points











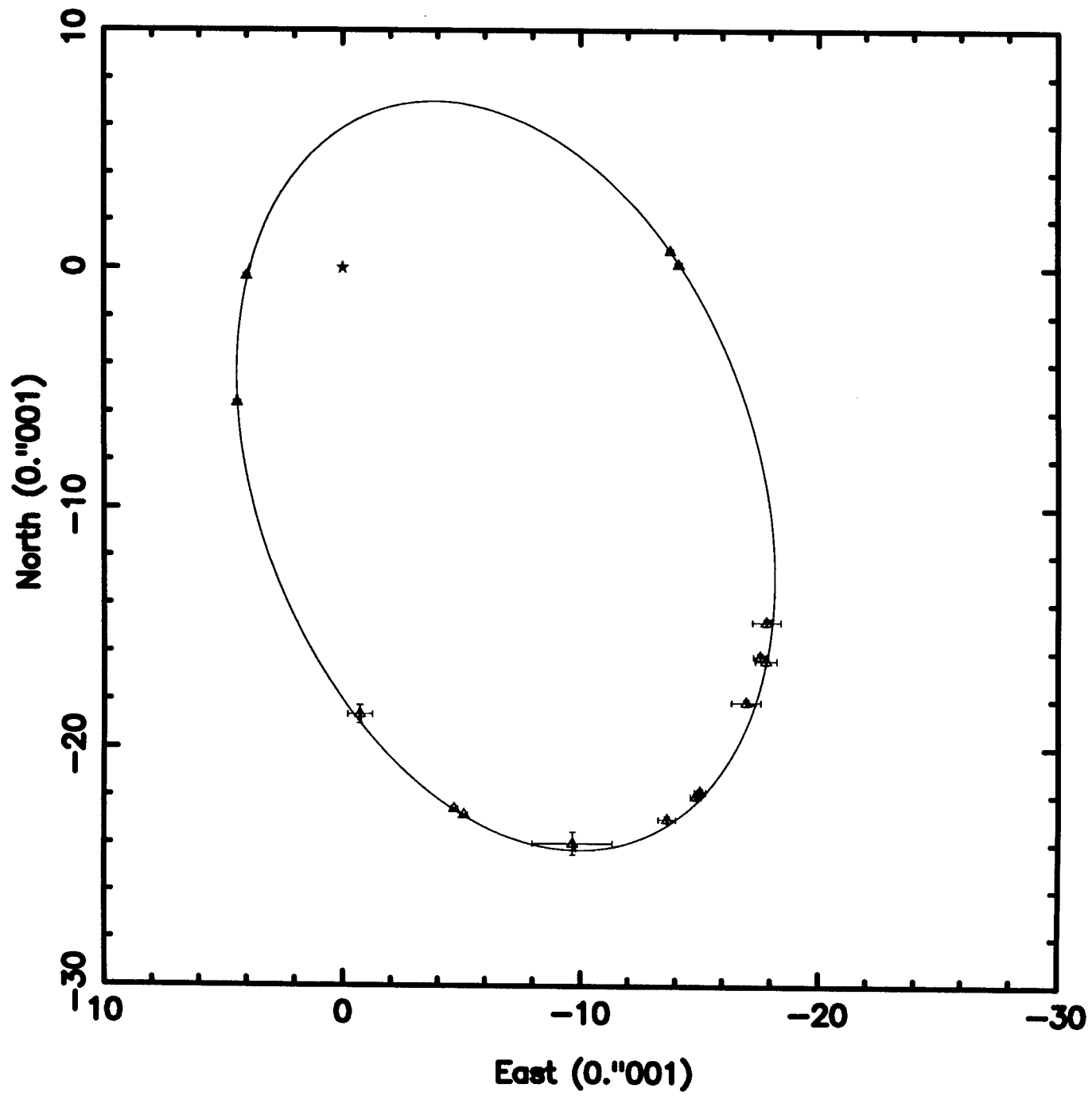


Table 1. Observation Log of  $\theta^2$  Tauri

JD 2400000+	baseline (m)	$\lambda$ ( $\mu\text{m}$ )	Scan
47791.9422	23.05	0.8,0.55,0.45	7
47805.9517	23.60	0.8,0.55,0.45	7
47826.9335	15.13	0.8,0.55,0.45	9
47831.9073	15.13	0.8,0.55,0.45	12
47832.9042	27.01	0.8,0.55,0.45	19
47836.8738	23.31	0.8,0.55,0.45	17
48189.9392	27.56	0.8,0.55,0.50	38
48233.8262	31.50	0.8,0.55,0.50	17
48234.8273	31.50	0.8,0.55,0.50	20
51104.9410	109.8	2.2	11
51105.9085	109.8	2.2	8
51127.8922	109.8	2.2	11
51130.8613	109.8	2.2	9
51154.7991	109.8	2.2	8
51155.8068	109.8	2.2	7

Table 2. Angular Separations of  $\theta^2$  Tauri (Equinox J2000.0)  
from interferometric observations and orbital calculations

JD 2400000+	$S_r(M)$ mas	$S_r(C)$ mas	$(M - C)_r$ mas	$S_d(M)$ mas	$S_d(C)$ mas	$(M - C)_d$ mas	$\rho$ mas	P.A. ( $^\circ$ )
47791.9422	-9.65	-9.80	0.15	-23.99	-24.32	0.33	25.86	201.91
47805.9517	-13.63	-13.71	0.08	-22.98	-23.26	0.28	26.72	210.67
47826.9335	-16.98	-17.41	0.43	-18.08	-18.20	0.12	24.80	223.20
47831.9073	-17.81	-17.86	0.05	-16.35	-16.49	0.14	24.18	227.45
47832.9042	-17.57	-17.93	0.36	-16.17	-16.13	-0.04	23.88	227.38
47836.8738	-17.83	-18.13	0.30	-14.75	-14.63	-0.12	23.14	230.40
48189.9392	-0.72	-0.70	-0.02	-18.62	-18.93	0.31	18.63	182.21
48233.8262	-14.85	-14.98	0.13	-22.01	-22.26	0.25	26.55	214.01
48234.8273	-15.03	-15.18	0.15	-21.82	-22.05	0.23	26.50	214.56
51104.9410	-14.13	-14.04	-0.09	0.15	0.36	-0.21	14.13	270.61
51105.9085	-13.77	-13.67	-0.10	0.72	0.88	-0.16	13.79	272.99
51127.8922	3.99	3.87	0.12	-0.37	0.19	-0.56	4.01	84.70
51130.8613	4.38	4.43	-0.05	-5.65	-5.24	-0.41	7.15	142.22
51154.7991	-4.70	-4.62	-0.08	-22.55	-22.56	0.01	23.03	191.77
51155.8068	-5.11	-5.01	-0.10	-22.80	-22.80	0.00	23.37	192.63

Table 3. Comparisons of Orbital Elements of  $\theta^2$ Tauri

	Spectroscopy								Interferometry	
	Ebbighausen (1959)		Peterson et al. (1993)		Tomkin et al. (1995)		Torres et al. (1997)		PTI & Mark III (1998)	
$P(\text{days})$	140.728	$\pm 0.004$	140.7308	$\pm 0.0020$	140.728	fixed	140.72816	0.00093	140.710	$\pm 0.015$
$T_0(\text{JD})$	36489.792	$\pm 0.129$	48171.02	$\pm 0.32$	49295.70	$\pm 0.14$	49015.32	$\pm 0.12$	50281.7	$\pm 0.12$
$e$	0.750	$\pm 0.006$	0.703	$\pm 0.011$	0.732	$\pm 0.005$	0.7266	$\pm 0.0049$	0.735	$\pm 0.005$
$a''(\text{mas})$	—	—	—	—	—	—	—	—	19.15	0.25
$i(^{\circ})$	—	—	—	—	—	—	—	—	47.3	0.9
$w(^{\circ})$	49.1	$\pm 1.3$	51.2	$\pm 1.8$	44.3	$\pm 1.4$	56.4	$\pm 1.1$	56.0	$\pm 1.2$
$\Omega(^{\circ})$	—	—	—	—	—	—	—	—	173.4	1.8

Note:

1.  $T_0$  is JD2400000+ value in columns

Table 4. Luminosities and Color Indices of  $\theta^2$  Tauri

Band (nm)	Both (mag)	$\Delta m$ (mag)	Primary (mag)	Secondary (mag)
450	$3.57 \pm 0.01$	$1.07 \pm 0.04$	$3.91 \pm 0.04$	$4.98 \pm 0.04$
V	$3.40 \pm 0.01$	$1.10 \pm 0.05$	$3.73 \pm 0.04$	$4.83 \pm 0.04$
800	$3.12 \pm 0.01$	$1.15 \pm 0.07$	$3.44 \pm 0.03$	$4.59 \pm 0.04$
K	$2.92 \pm 0.01$	$1.20 \pm 0.03$	$3.25 \pm 0.03$	$4.37 \pm 0.03$
450-V	$0.18 \pm 0.01$	—	$0.18 \pm 0.01$	$0.15 \pm 0.01$
V-800	$0.27 \pm 0.01$	—	$0.29 \pm 0.02$	$0.22 \pm 0.02$
V-K	$0.47 \pm 0.01$	—	$0.48 \pm 0.02$	$0.46 \pm 0.02$

Table 5. Comparisons between Lunar Occultation and Interferometry

	Lunar Occultation		Interferometry
	Evans et al. (1980)	Peterson et al. (1981)	PTI & Mark III (this work)
Separation (mas)	11.3±0.3	—	13.2±0.2
	11.8±0.6	—	13.2±0.2
	—	20.77±0.15	19.9±0.2
$\Delta m$ (mag)	0.61±0.09 (467nm)	1.07±0.04 (440nm)	1.16±0.13 (450nm)
	0.96±0.17 (547nm)	1.18±0.05 (630nm)	1.18±0.10 (550nm)
	—	1.04±0.06 (790nm)	1.15±0.07 (800nm)
	—	—	1.12±0.03 (2.2 $\mu$ m)